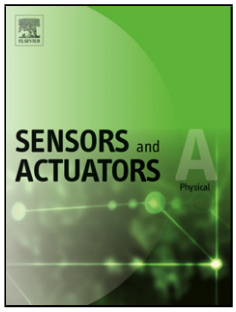

Title: Flexible carbon nanotube nanocomposite sensor for multiple physiological parameter monitoring

Author: Anindya Nag Subhas Chandra Mukhopadhyay
Jürgen Kosel

PII: S0924-4247(16)30707-5
DOI: http://dx.doi.org/doi:10.1016/j.sna.2016.10.023
Reference: SNA 9879

To appear in: *Sensors and Actuators A*

Received date: 30-5-2016
Revised date: 13-10-2016
Accepted date: 14-10-2016

Please cite this article as: Anindya Nag, Subhas Chandra Mukhopadhyay, Jürgen Kosel, Flexible carbon nanotube nanocomposite sensor for multiple physiological parameter monitoring, Sensors and Actuators: A Physical http://dx.doi.org/10.1016/j.sna.2016.10.023

Flexible carbon nanotube nanocomposite sensor for multiple physiological parameter monitoring

Anindya Nag[1*], Subhas Chandra Mukhopadhyay[1], Jürgen Kosel[2]

[1]Faculty of Science and Engineering
Macquarie University
Sydney, NSW, Australia.

*Corresponding author email: anindya1991@gmail.com
[2]Computer, Electrical, Mathematical, Science and Engineering Division
King Abdullah University of Science and Technology (KAUST)
Saudi Arabia.

Highlights:

- Novel flexible, strain-sensitive sensor prototypes were fabricated for multiple physiological parameter monitoring.
- The sensor patch was made of Polydimethylsiloxane (PDMS) as the substrate and a thin layer of a nanocomposite comprising of PDMS and functionalized multi-walled carbon nanotubes (MWCNTs) as electrodes.
- Laser cutting was done to design the electrodes.
- The novelty lies in the material and structural aspect.
- The sensor patch was used for monitoring limb movements and respiration.

Abstract— **The paper presents the design, development, and fabrication of a flexible and wearable sensor based on carbon nanotube nanocomposite for monitoring specific physiological parameters. Polydimethylsiloxane (PDMS) was used as the substrate with a thin layer of a nanocomposite comprising functionalized multi-walled carbon nanotubes (MWCNTs) and PDMS as electrodes. The sensor patch functionalized on strain-sensitive capacitive sensing from interdigitated electrodes which were patterned with a laser on the nanocomposite layer. The thickness of the electrode layer was optimized regarding strain and conductivity. The sensor patch was connected to a monitoring device from one end and attached to the body on the other for examining purposes. Experimental results show the capability of the sensor patch used to detect respiration and limb movements. This work is a stepping stone of the sensing system to be developed for multiple physiological parameters.**

Keywords— PDMS, carbon nanotubes, nanocomposite, sensor patch, respiration, limb movement.

1. Introduction

The development of a novel flexible sensor patch for sensing multiple parameters is described in this paper. The sensor patch utilizes polydimethylsiloxane (PDMS) as the substrate and a nanocomposite of PDMS and carbon nanotubes (CNT) as electrodes. PDMS had been substantially used [1-3] for the development of flexible sensors due to its low cost, non-toxicitiy, inertness and hydrophobic nature. CNTs were preferred as the conducting material over other metallic nanowires because of their biocompatibility, high flexibility, resistance towards temperature change, low stiffness, and high tensile strength.
Multi-walled carbon nanotubes (MWCNTs) were used for the experiments functionalized with carboxylic groups (-COOH). The functionalized MWCNTs have a better dispersing capability inside a polymer compared to unfunctionalized or single-walled carbon nanotubes (SWCNT). This leads to a better interfacial bonding between the nanotubes and the polymer resulting in a higher conductivity. Interdigitated electrodes were patterned on the nanocomposite layer, allowing for a non-invasive and single-sided strain measurement. The patterns were produced using CO_2 laser ablation [4, 5]. Compared to other fabrication techniques like 3-D printing [6], photolithography [7], inkjet printing [8], etc., it excels at the ease of sample preparation without the need for any templates or additional material. This method fabricates very thin and flexible materials and can cut smooth edges which are approxmiately parperdicular to the surface. By attaching the sensor to the skin, respiration and limb movements were tested on different people as shown in the experimental results section, to verify its functionality.
The concept of sensors to monitor people's health and lifestyle has been capitalized since the past two decades [9, 10]. Different types of sensors have been used to monitor the activities and physiological parameters of the individuals to understand and generate a pattern for human behavior [11-13]. Sensors with flexible substrates are one sector where prominent research work [14-17] has been done in recent times. Light weight, low cost of fabrication, long lasting capability are some of the reasons for their increased usage over rigid substrates. The sensors developed for smart home usage are mainly dedicated for single parameter monitoring purposes like PIR sensors [18], pressure sensors, etc.
Multiparameter monitoring is of great interest due to the disadvantage caused by sensors for individual applications. For example, the cost is largely reduced in using a multi-functional sensor. The sensor patch development shown in this paper is much simpler and easier to fabricate compared to previously developed sensors, which had been fabricated for multiple functions containing a coil [19-21] operating on a magnetic principle.
Significant research work has also been done on the detection of joint and limb movements. The majority of them involves fixed sensors [22] or the study of an artificial robot [23] to analyze the human behavior. Wearable sensors [24] and accelerometers [25] are other techniques used to monitor human movement. Shoe sensors [26] and braces [27] are some types of wearable sensors used for monitoring of physical activities involving limb movements. The existing concepts have distinct disadvantages. Some

would be wearable sensing devices required to be worn by the person at times; others would involve complicated gadgets working on specific computational algorithms involving an expertise to operate them. Thus, there is a need for a simple, non-invasive, sensing device which upon its attachment to the monitored region would precisely detect the movements, even on a smaller scale. Research work to monitor the rate of respiration has been done previously using devices with and without flexible substrates. The photoplethysmographic technique [28, 29] is widely used for the detection of respiratory rate. But this technique is complex and requires technicians at the time of monitoring. Piezo-resistive [30], fabric attached sensing [31, 32] and optical sensors [33] are other ways used to monitor respiratory rate. Technical complexity, cost and specific positioning of the subject during monitoring are some of the demerits of these techniques. Monitoring of respiration and other physiological parameters has also been done using PVDF-based piezoelectric sensors [34, 35]. But the disadvantages of using PDVF are the strong temperature depending performance along with high hysteresis exerted by the sensors. There are different force sensors available in the market. Table 1 classifies them based on price, size and some applications related to physiological parameter monitoring. Typically, either the price of the sensors is very high or the sensor size is large. In this paper, we show the change in capacitance of an interdigitated electrode on a flexible sensor patch by simply attaching it to the lower part of the diaphragm of an individual. The inhalation and exhalation rates were monitored based on the strain induced on the sensor patch. This could be used for applications like the abnormality in the rate of respiration caused due to hypoxemia and hyperemia which can be analyzed by monitoring the change in sensor capacitance between a healthy person and a patient.

2. Theory

The working principle of the sensor is based on the deformation of an interdigital electrode structure. The capacitance of any parallel plate capacitive device can be generally expressed by,

$$C = {(\in_o * \in_r * A)}/{d} \quad (1)$$

where,
C is the capacitance of the interdigital sensor,
$\in_o = 8.85$ *is the* $\times 10^{-12}$ $F{\cdot}m^{-1}$ *is the permittivity of vacuum,*
$\in_r$ *is the relative permittivity,*
A is the effective area, and
d is the effective spacing between electrodes of different polarity.

A change of d or A causes a change of the capacitance. This can be exploited to monitor a physiological event through the change in capacitance based on the deformation-reformation of the sensor patch. The exertion of tensile stress on the patch via a physiological event changes the capacitance with respect to its normal position [36, 37]. Fig. 1 depicts the notion. L and W stand for the length and width of the sensor patch, respectively. ΔL, ΔW, and Δd are the changes in length, width and interdigital distance of the sensor patch, respectively, caused when deformed. Using equation (1), the change in capacitance can be calculated as a function of change in length (ΔL), width (ΔW) and interdigital distance (Δd) as shown in equation (2).

$$\Delta C = f\,(\Delta L, \Delta W, \Delta d) \quad (2)$$

3. Fabrication and Characterization of the Sensor Patch

The schematic diagram of the fabrication steps is given in fig. 2. PDMS (SYLGARD ® 184, Silicon Elastomer Base) was cast at a ratio of 10:1 of base elastomer (pre-polymer) and curing agent (cross-linker) on a Poly (methyl methacrylate) (PMMA) template. The template was patterned using a laser cutter (Universal Laser Systems). PMMA was chosen because of its impassiveness towards PDMS and the cured material can be easily peeled off from the base without any additional steps. The thickness of the cast PDMS was adjusted to 1 mm by a casting knife (SHEEN, 1117/1000 mm). The sample was then desiccated for 2 hours to remove any trapped air bubbles.

The sample was cured at 80^0 C for 8 hours to form the substrate for the sensor patch. A mixture consisting of functionalized MWCNTs (Aldrich, 773840-100G) and PDMS was then cast onto the cured PDMS. 4 % wt. of CNT was used after an optimization between the conductivity and dispersion of CNT into PDMS. Followed by the adjustment of the thickness of the nanocomposite layer by the casting knife to around 600 µm, the sample was again desiccated for 2 hours to remove any trapped air bubbles. Then the nanocomposite layer was cured at 80^0 C for 8 hours. Laser induction (Universal Laser Systems) was then

employed to form the electrodes pattern on the cured nanocomposite. A SEM image of the nanocomposite is shown in fig. 3. The white regions as shown in the image are the PDMS, and their counterpart black regions are the CNTs.

Images of the individual steps are shown in fig. 4. Table 2 shows the combination of power and speed settings tried for an optimal cut of the sensor patch. Power (W) refers to the how energetically the laser fires on the sample. Speed (m/min) refers to the rate of movement of the laser nozzle in X and Y directions. Z-axis was used to adjust the focal point of the laser beam on the ablated material. This is done by moving the laser head in the z-direction. The thicknesses of the electrodes were measured by a profilometer (XP-200). While fabricating sensors with very low power and speed settings, a hardening effect on the patch was observed, this led to the nanocomposite to come off upon application of stress to the patch. After a series of short-circuit and transparency tests on the different electrodes, the one fabricated with a combination of the power of 24 W and speed of 70 m/min turned out to be the most viable one and was used for further characterization and experimentation. The front and rear views of the sensor patch are shown in fig. 5. The black spots in the PDMS shown in the rear view of the sensor patch are some agglomeration of CNTs that lie within the PDMS layer.

Impedance measurements of the sensor patch were performed by a Precision Impedance Analyzer (Agilent 4294A). Open and short calibrations were done before measurements to remove the effect of stray capacitances. The frequency was swept from 10 kHz to 10 MHz, and the impedances (Z) and phase angles (Θ) recorded are shown in figs. 6 and 7. The sensor patch is capacitive in its nature with the largest phase angle observed at 150 kHz. Hence, further characterization was conducted at the operating frequency of 150 kHz.

The stress-strain relationship of the sensor patch was determined using an INSTRON extensometer tensile/compressive force testing system (VS02477052 R: F). Stresses applied to the horizontal and vertical direction to the sensor patch are shown in fig. 8. As can be seen from fig. 9, an expected stress-strain relationship [38] is followed in the horizontal direction compared to the vertical direction. This could be due to the anisotropic geometry of the electrodes. The fracture points for the tensile stress were (1420 µm, 2060 mN) and (-1680 µm, -840 mN). The lower limit of negative strain was caused due to the excessive bending of the patch. The capacitance-strain relationship of the patch is shown in fig. 10. The sensor showed a prominent change in capacitance at the operating frequency (150 kHz). The sensitivity is calculated from the curve with the optimum frequency of 150 kHz.

$$\text{Sensitivity} = \frac{\Delta C}{\Delta Strain} = \frac{179.2 - 122.3}{1187.5 - 728} = 0.124\ pF/\mu m.$$

The linear region of the frequency line is from 610 µm to 1120 µm. The saturation strain at the operating frequency curve (150 kHz) is 2160 µm.

4. Experimental Set-up

To test the sensor for biophysical parameter monitoring, the patch was attached to the skin using biocompatible tapes (VHB 3M RP) as shown in fig. 11. The sensor was attached only after the skin was completely dried to minimize the effect of sweat or water on the attachment of the tapes. The presence of sweat would lead to an additional capacitive layer between the sensor and skin leading to erroneous results. The measurements of the change in capacitance of the sensor were done by a Precision LCR meter (E4980A) at 150 kHz. BNC to alligator clips were used to connect the instrument to the sensor patch which was attached to the body. Respiratory measurements were done by attaching the sensor at the lower end of the diaphragm. The readings were taken for two different conditions. The sensor was attached to the trochlea elbow and the patella of the knee to detect the movement of limbs. The terms ‘flexed’ and ‘extended’ shown in the figures refer to the states of the limb position. The arms were moved from a fully extended position, i.e., resting on the table to a fully flexed position via bending the elbow. The leg movement was done in a similar fashion by bending the knee from an extended to a flexed position. The sensor position on the body is crucial regarding the life span and reproducibility of the results. For example, if the sensor is placed in a tilted position, the stress exerted on the patch would not be distributed equally. This would stretch the patch non-uniformly generating an unequal interdigital distance (d) between the electrodes, producing erroneous results. Fig. 12 shows images of the experiments for monitoring of limb movement and respiration.

5. Experimental Results and Discussion

People of different age groups were tested for monitoring limb movements and respiration to validate the functionality of the sensor patch. Figs. 12-15 show the sensor output when the subject was at rest and the limbs were moved in an oscillatory fashion. The results show that limb movements can be clearly detected with the sensor patch. The limbs were flexed up to the angle of 140^0, considering the extended limb to be zero degrees. There are a few issues that can be addressed to optimize the performance. For example, in figs. 12 and 13, fluctuations are observed, during the flexed state. This can lead to contradictory assumptions of

the state of the limb. The reason for could be the movement of the cables. This issue would be addressed by the wireless operation. Movements of the limbs loosened the sensor patch from the skin, leading to the observed artifacts. The signals in the flexed position showed to some extent different values. The reason for this is that the movement of the limbs was not completely identical for two different situations.

Figs. 16-17 show the sensor output when the person is at motion. The change in capacitance was monitored when the person moved his limbs while walking. Not much difference is found in this case compared to the output when the subject is at rest. The difference between the two situations, flexed and extended, can still easily be distinguished. The different angular change on a reference of a limb of a subject is shown in fig. 18. The measurements were taken using a Winkletronic angle finder (450 mm). This experiment was performed to determine a relation between the changes in capacitance on each degree movement of the limb. It is seen from fig. 19 that the sensor patch's change of capacitance is linear with the degree of movement of the limbs. The angular variation of the limbs was considered up to 130^0 because the limbs do not bend further with respect to the reference.

Fig. 20 shows the output of the sensor when used for the detection of respiratory activity. The reading shown in two colors defines two different individuals. Fig. 21 depicts the different rate of respiration signals. The contraction and expansion happening to the sensor patch simultaneously with the movement of the diaphragm caused a change in inter-electrode distance (d) and area (A) of the sensing surface of the sensor. Hence, the sensor patch can precisely differentiate the different rates of inhalation and exhalation by a prominent change in capacitance. The inhale and exhale rates were also varied in a controlled fashion to further analyze the sensitivity of the sensor patch as shown in fig. 22.

6. Conclusion and Future Work

Functionalized MWCNTs as conductive material embedded in a PDMS substrate based flexible sensor for multiple physiological parameters monitoring has been designed and fabricated. The MWCNTs were chosen as filler for nanocomposite due to their high electrical conductivity and flexibility along with their aspect ratio. The functionalization groups like C-OOH, C-O and other oxygen carboxyl groups helped in increasing electrical conductivity and allowed better dispersion of the nanotubes in the polymer [39]. PDMS provides a low Young's modulus, required for a high-performance patch in terms of strain range and durability. It is also cheap compared to other polymers (Polyethylene naphthalate, Polyethylene terephthalate) used commonly to develop flexible sensors. Due to their hydrophobicity, PDMS as a sensor substrate minimizes the effects of sweat on the sensor output and attachment. The size of the sensor is small, around $50mm^2$, making it convenient to use for monitoring physiological parameters of elderly people or infants by minimizing discomfort. The developed patch was used for non-invasive monitoring of multiple physiological parameters. Respiration measurements of different individuals along with limb movements were monitored by attaching the sensor to the skin of the moving body parts. A particular advantage of this method is the potential of multiple parameters sensing ability, thus reducing the number of sensors required for the individual parameter, making it practical and cost efficient.

Acknowledgement

The authors would like to thank King Abdullah University of Science and Technology, Saudi Arabia, for providing the research facilities to design and fabricate the sensor patches. They would also thank Massey University, Palmerston North for providing the conditions to test the patches. They are also obliged to the people volunteered during the testing of the sensor patch.

References

[1] D. Armani, C. Liu, N. Aluru, Re-configurable fluid circuits by PDMS elastomer micromachining, Micro Electro Mechanical Systems, 1999 MEMS'99 Twelfth IEEE International Conference on, Ieee1999, pp. 222-7.
[2] T. Fujii, PDMS-based microfluidic devices for biomedical applications, Microelectronic Engineering, 61(2002) 907-14.
[3] B.-H. Jo, L.M. Van Lerberghe, K.M. Motsegood, D.J. Beebe, Three-dimensional micro-channel fabrication in polydimethylsiloxane (PDMS) elastomer, Microelectromechanical Systems, Journal of, 9(2000) 76-81.
[4] M.C. Gower, Excimer laser microfabrication and micromachining, First International Symposium on Laser Precision Microfabrication (LPM2000), International Society for Optics and Photonics2000, pp. 124-31.
[5] D. Snakenborg, H. Klank, J.P. Kutter, Microstructure fabrication with a CO2 laser system, Journal of Micromechanics and microengineering, 14(2004) 182.
[6] C.X.F. Lam, X. Mo, S.-H. Teoh, D. Hutmacher, Scaffold development using 3D printing with a starch-based polymer, Materials Science and Engineering: C, 20(2002) 49-56.
[7] N. Herzer, S. Hoeppener, U.S. Schubert, Fabrication of patterned silane based self-assembled monolayers by photolithography and surface reactions on silicon-oxide substrates, Chemical Communications, 46(2010) 5634-52.
[8] B.-J. De Gans, P.C. Duineveld, U.S. Schubert, Inkjet printing of polymers: state of the art and future developments, Advanced materials, 16(2004) 203-13.
[9] B. Najafi, K. Aminian, A. Paraschiv-Ionescu, F. Loew, C.J. Büla, P. Robert, Ambulatory system for human motion analysis using a kinematic sensor: monitoring of daily physical activity in the elderly, Biomedical Engineering, IEEE Transactions on, 50(2003) 711-23.
[10] K. Altun, B. Barshan, Human activity recognition using inertial/magnetic sensor units, Human behavior understanding, Springer2010, pp. 38-51.
[11] K. Malhi, S.C. Mukhopadhyay, J. Schnepper, M. Haefke, H. Ewald, A Zigbee-based wearable physiological parameters monitoring system, Sensors Journal, IEEE, 12(2012) 423-30.
[12] S.D.T. Kelly, N.K. Suryadevara, S.C. Mukhopadhyay, Towards the implementation of IoT for environmental condition monitoring in homes, Sensors Journal, IEEE, 13(2013) 3846-53.
[13] N.K. Suryadevara, S.C. Mukhopadhyay, Wireless sensor network based home monitoring system for wellness determination of elderly, Sensors Journal, IEEE, 12(2012) 1965-72.
[14] A. Arena, N. Donato, G. Saitta, A. Bonavita, G. Rizzo, G. Neri, Flexible ethanol sensors on glossy paper substrates operating at room temperature, Sensors and Actuators B: Chemical, 145(2010) 488-94.
[15] C. Ashruf, Thin flexible pressure sensors, Sensor Review, 22(2002) 322-7.
[16] D. Briand, F. Molina-Lopez, A.V. Quintero, C. Ataman, J. Courbat, N.F. de Rooij, Why going towards plastic and flexible sensors?, Procedia engineering, 25(2011) 8-15.
[17] C. Charton, N. Schiller, M. Fahland, A. Holländer, A. Wedel, K. Noller, Development of high barrier films on flexible polymer substrates, Thin Solid Films, 502(2006) 99-103.
[18] T.L. Hayes, S. Hagler, D. Austin, J. Kaye, M. Pavel, Unobtrusive assessment of walking speed in the home using inexpensive PIR sensors, Engineering in Medicine and Biology Society, 2009 EMBC 2009 Annual International Conference of the IEEE, IEEE2009, pp. 7248-51.
[19] H. Pfützner, E. Kaniusas, J. Kosel, L. Mehnen, T. Meydan, M. Vázquez, et al., Magnetostrictive bilayers for multi-functional sensor families, Sensors and Actuators A: Physical, 129(2006) 154-8.
[20] L. Mehnen, E. Kaniusas, J. Kosel, J. Téllez-Blanco, H. Pfützner, T. Meydan, et al., Magnetostrictive bilayer sensors—a survey, Journal of alloys and compounds, 369(2004) 202-4.
[21] E. Kaniusas, H. Pfützner, L. Mehnen, J. Kosel, J.C. Téllez-Blanco, G. Varoneckas, et al., Method for continuous nondisturbing monitoring of blood pressure by magnetoelastic skin curvature sensor and ECG, Sensors Journal, IEEE, 6(2006) 819-28.
[22] V.M. Crabtree, A. Ivanenko, L.M. O'Brien, D. Gozal, Periodic limb movement disorder of sleep in children, Journal of Sleep Research, 12(2003) 73-81.
[23] K. Aminian, B. Najafi, Capturing human motion using body-fixed sensors: outdoor measurement and clinical applications, Computer Animation and Virtual Worlds, 15(2004) 79-94.
[24] K.D. Nguyen, I. Chen, Z. Luo, S.H. Yeo, H.B.-L. Duh, A wearable sensing system for tracking and monitoring of functional arm movement, Mechatronics, IEEE/ASME Transactions on, 16(2011) 213-20.
[25] C.-C. Yang, Y.-L. Hsu, A review of accelerometry-based wearable motion detectors for physical activity monitoring, Sensors, 10(2010) 7772-88.
[26] E.S. Sazonov, G. Fulk, J. Hill, Y. Schutz, R. Browning, Monitoring of posture allocations and activities by a shoe-based wearable sensor, Biomedical Engineering, IEEE Transactions on, 58(2011) 983-90.
[27] J. Bell, X. Shen, E. Sazonov, Early detection of sit-to-stand transitions in a lower limb orthosis, Engineering in Medicine and Biology Society (EMBC), 2015 37th Annual International Conference of the IEEE, IEEE2015, pp. 5028-31.
[28] P.A. Leonard, J.G. Douglas, N.R. Grubb, D. Clifton, P.S. Addison, J.N. Watson, A fully automated algorithm for the determination of respiratory rate from the photoplethysmogram, Journal of Clinical Monitoring and Computing, 20(2006) 33-6.
[29] L. Nilsson, A. Johansson, S. Kalman, Monitoring of respiratory rate in postoperative care using a new photoplethysmographic technique, Journal of Clinical Monitoring and Computing, 16(2000) 309-15.
[30] T. Reinvuo, M. Hannula, H. Sorvoja, E. Alasaarela, R. Myllylä, Measurement of respiratory rate with high-resolution accelerometer and EMFit pressure sensor, Sensors Applications Symposium, 2006 Proceedings of the 2006 IEEE, IEEE2006, pp. 192-5.
[31] S. Jung, T. Ji, V.K. Varadan, Point-of-care temperature and respiration monitoring sensors for smart fabric applications, Smart materials and structures, 15(2006) 1872.
[32] C.R. Merritt, H.T. Nagle, E. Grant, Textile-based capacitive sensors for respiration monitoring, IEEE Sensors journal, 9(2009) 71-8.
[33] M. Warkentin, H.M. Freese, U. Karsten, R. Schumann, New and fast method to quantify respiration rates of bacterial and plankton communities in freshwater ecosystems by using optical oxygen sensor spots, Applied and environmental microbiology, 73(2007) 6722-9.
[34] N. Bu, N. Ueno, O. Fukuda, Monitoring of respiration and heartbeat during sleep using a flexible piezoelectric film sensor and empirical mode decomposition, 2007 29th Annual International Conference of the IEEE Engineering in Medicine and Biology Society, IEEE2007, pp. 1362-6.
[35] Y.-Y. Chiu, W.-Y. Lin, H.-Y. Wang, S.-B. Huang, M.-H. Wu, Development of a piezoelectric polyvinylidene fluoride (PVDF) polymer-based sensor patch for simultaneous heartbeat and respiration monitoring, Sensors and Actuators A: Physical, 189(2013) 328-34.
[36] R. Matsuzaki, A. Todoroki, Wireless flexible capacitive sensor based on ultra-flexible epoxy resin for strain measurement of automobile tires, Sensors and Actuators A: Physical, 140(2007) 32-42.
[37] L. Cai, L. Song, P. Luan, Q. Zhang, N. Zhang, Q. Gao, et al., Super-stretchable, transparent carbon nanotube-based capacitive strain sensors for human motion detection, Scientific reports, 3(2013).

[38] S. Frankland, V. Harik, G. Odegard, D. Brenner, T. Gates, The stress–strain behavior of polymer–nanotube composites from molecular dynamics simulation, Composites Science and Technology, 63(2003) 1655-61.
[39] C.H. Lau, R. Cervini, S.R. Clarke, M.G. Markovic, J.G. Matisons, S.C. Hawkins, et al., The effect of functionalization on structure and electrical conductivity of multi-walled carbon nanotubes, Journal of Nanoparticle Research, 10(2008) 77-88.

AUTHORS' BIOGRAPHIES

MR. ANINDYA NAG HAS COMPLETED BACHELOR OF TECHNOLOGY FROM WEST BENGAL UNIVERSITY OF TECHNOLOGY (WBUT), INDIA IN 2013 AND MASTER OF ENGINEERING (M.E.) AT MASSEY UNIVERSITY, PALMERSTON NORTH, NEW ZEALAND IN JUNE 2015. HIS RESEARCH INTERESTS ARE IN THE AREA OF SMART SENSORS AND SENSING TECHNOLOGY FOR HOME AND ENVIRONMENTAL MONITORING. HE IS CURRENTLY PURSUING PH.D. IN ENGINEERING AT MACQUARIE UNIVERSITY, AUSTRALIA. HE IS WORKING ON "PRINTED FLEXIBLE SENSORS FOR HUMAN WELLNESS."

Dr. Subhas Chandra Mukhopadhyay (M'97, SM'02, F'11) is working as a Professor of Mechanical/Electronics Engineering with the Department of Engineering, Macquarie University, Australia. He is a Fellow of IEEE (USA), a Fellow of IET (UK). He is a Topical Editor of IEEE Sensors Journal, an Associate Editor of IEEE Transactions on Instrumentation and Measurements. He was a Distinguished Lecturer of IEEE Sensors Council from 2010-2013. He chairs the IEEE IMS Technical Committee 18 on Environmental Measurements.

Dr. Jurgen Kosel is Associate Professor of Electrical Engineering at the King Abdullah University of Science and Technology (KAUST), Thuwal, Saudi Arabia, and head of the Sensing, Magnetism and Microsystems Research Group. He was a post-doctoral fellow with the Biomedical Engineering Research Group, Stellenbosch University, South Africa, from 2007 to 2009. From 2006 to 2007, he worked in the automotive industry as a Project Manager with Magna Powertrain, Graz, Austria. He received the Dipl.-Ing. (M.Sc.) and Ph.D. degrees in electrical engineering from the Vienna University of Technology, Vienna, Austria, in 2002 and 2006, respectively. His research interests are in the fields of Micro and Nanodevices with a focus on magnetic transducers.

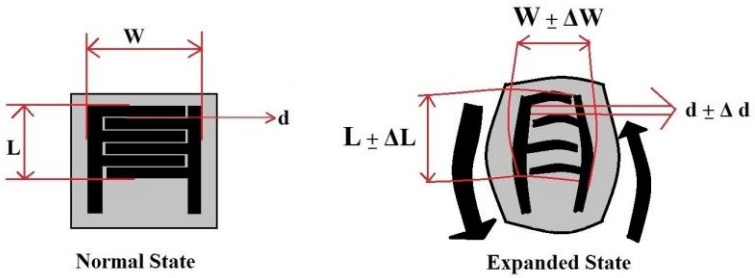

Fig. 1: Schematic design of the sensor patch made of a flexible PDMS substrate (gray) with electrodes made of a carbon nanotube/ PDMS nanocomposite (black). Straining the sensor patch leads to a change of the sensor's length (L) and width (w) as well as the electrode distance d, resulting in a change of the measured capacitance value.

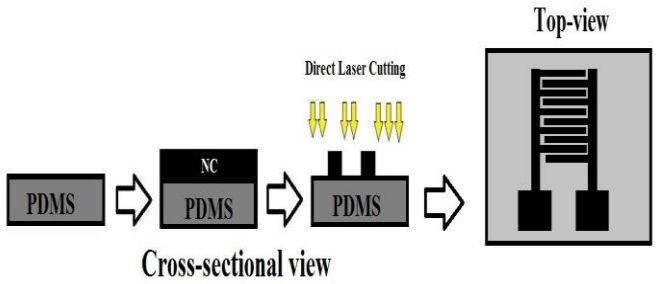

Fig. 2: Schematic diagram of the fabrication steps.
PDMS: Polydimethylsiloxane. NC: Nanocomposite.

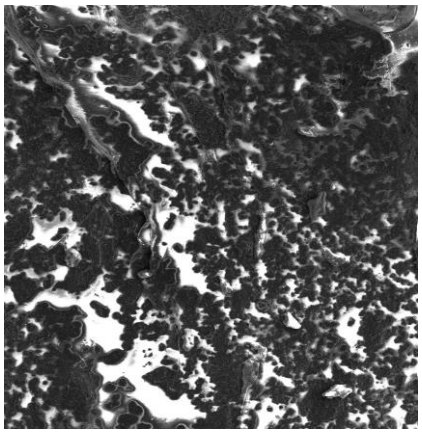

Fig. 3: SEM top-view image of the nanocomposite consisting of CNTs (4% wt.) and PDMS.

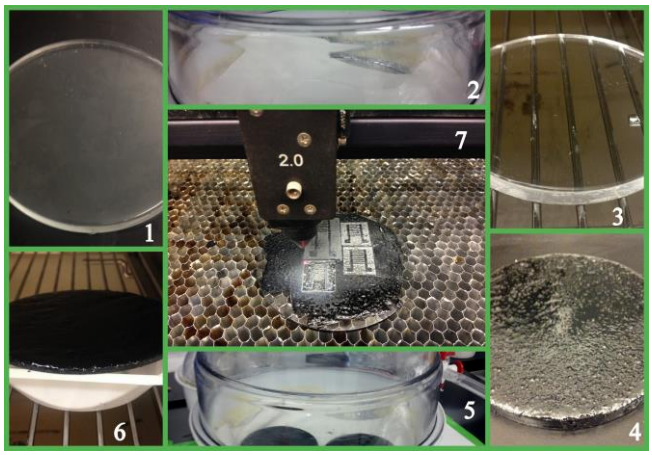

Fig. 4: Fabrication steps: (1) Casting of PDMS (2) Desiccation of PDMS (3) Curing of PDMS (4) Casting of nanocomposite (NC) (5) Desiccation of NC (6) Curing of NC (7) Laser patterning of electrodes.

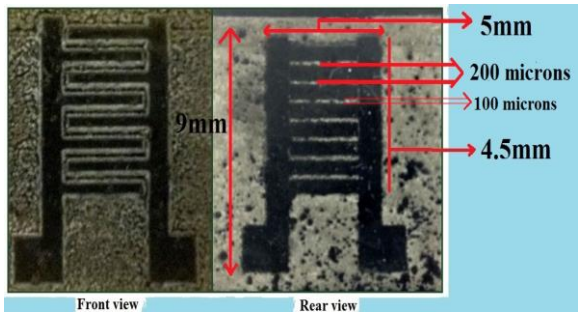

Fig. 5: Front and rear view images of the sensor patch.

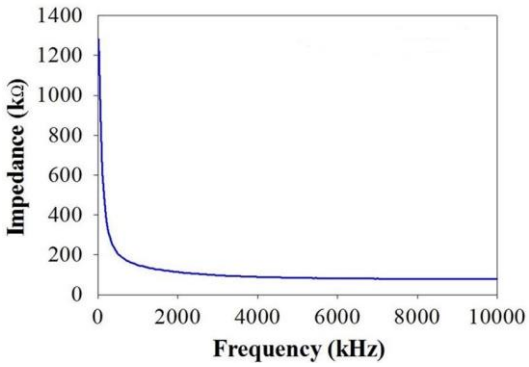

Fig. 6: Impedance behavior of the sensor patch as a function of frequency.

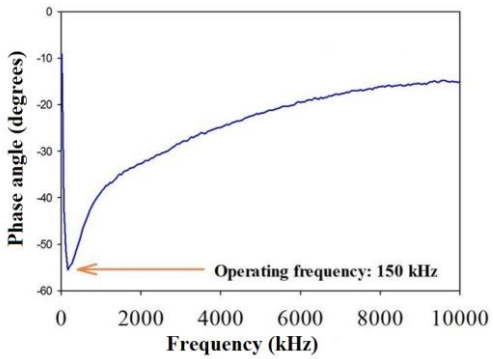

Fig. 7: Phase-angle of the sensor patch as a function of frequency.

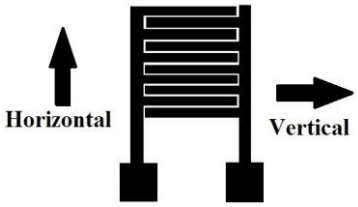

Fig. 8: Directions of the applied stresses for the stress/strain characterization of the sensor patch.

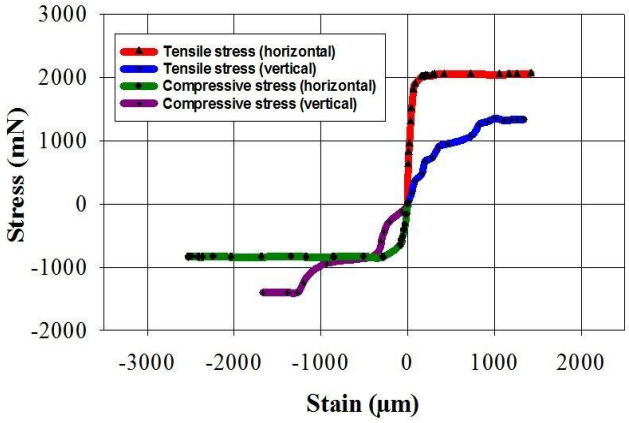

Fig. 9: Stress-strain relationship of the sensor patch.

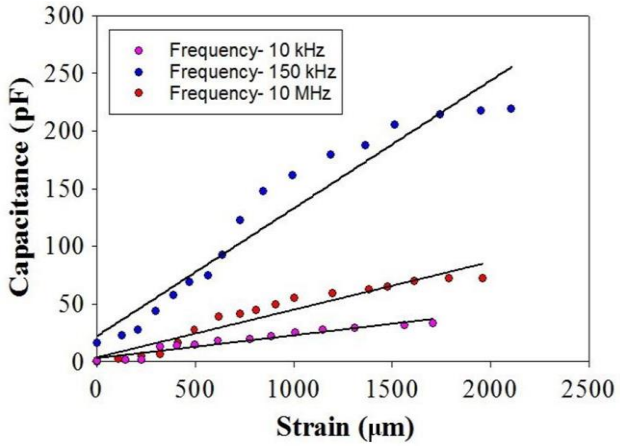

Fig. 10: Relation between capacitance and strain of the sensor patch in the horizontal direction.

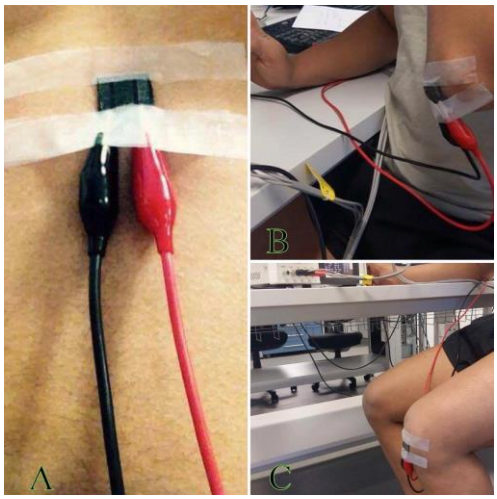

Fig. 11: Sensor attachment for the biophysical parameters: (A): Monitoring of respiration with the sensor attached on the lower part of the diaphragm. (B): Sensor attached on the elbow to monitor the arm movement. (C): Sensor attached on the knee to monitor the leg movement.

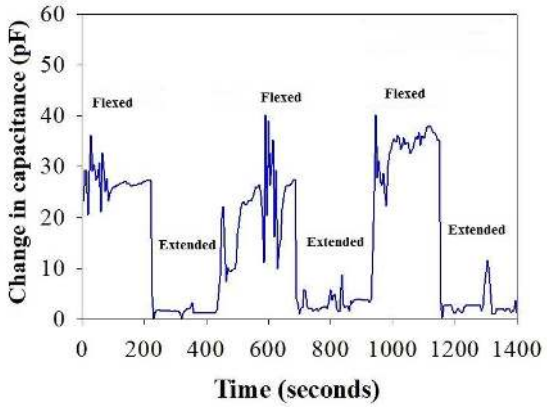

Fig. 12: Detection of left arm movement when the subject is at rest.

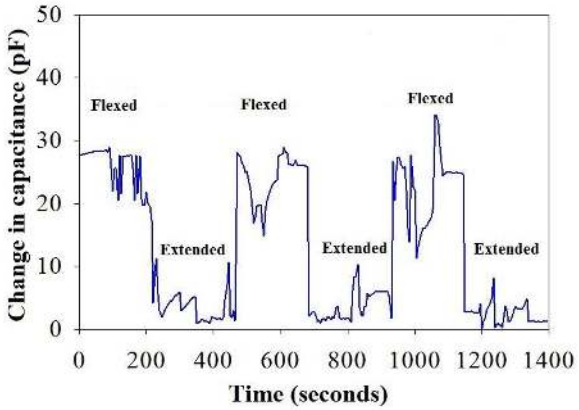

Fig. 13: Detection of right arm movement when the subject is at rest.

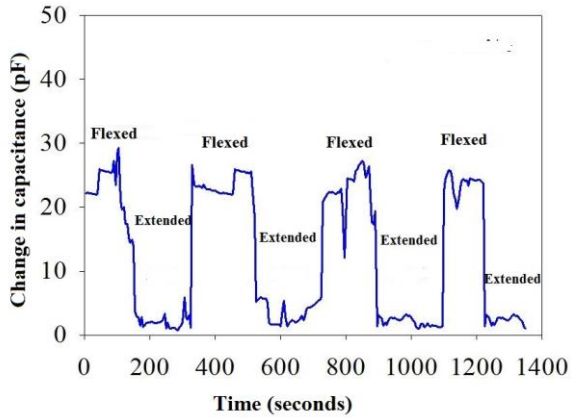

Fig. 14: Detection of left leg movement when the subject is at rest.

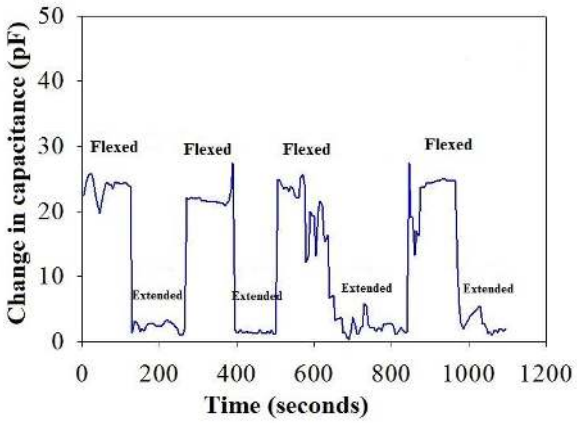

Fig. 15: Detection of right leg movement when the subject is at rest.

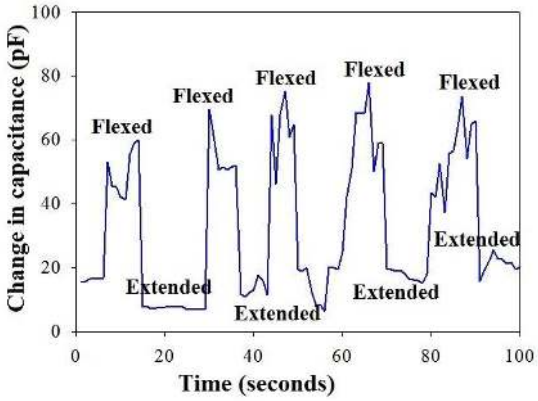

Fig. 16: Detection of right arm movement when the subject is at motion.

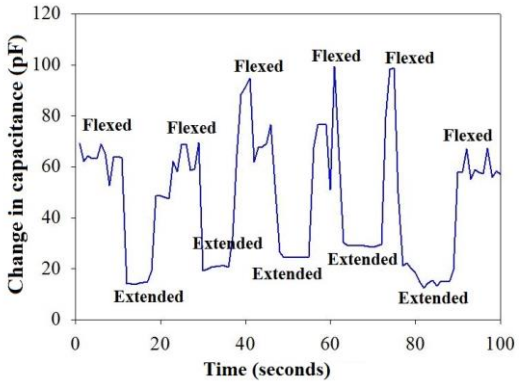

Fig. 17: Detection of right leg movement when the subject is at motion.

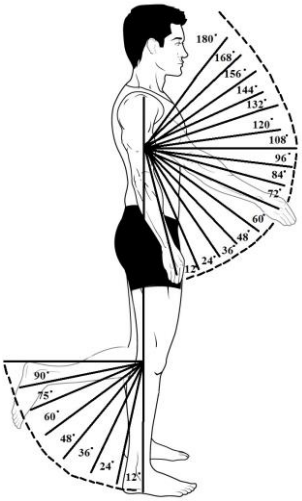

Fig. 18: Different angular measurements of the limbs of a subject.

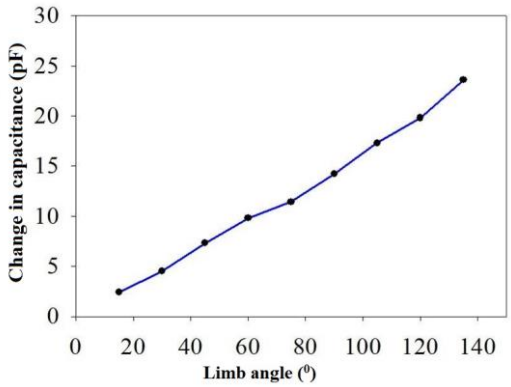

Fig. 19: Change of capacitance as a function of the right arm limb movement.

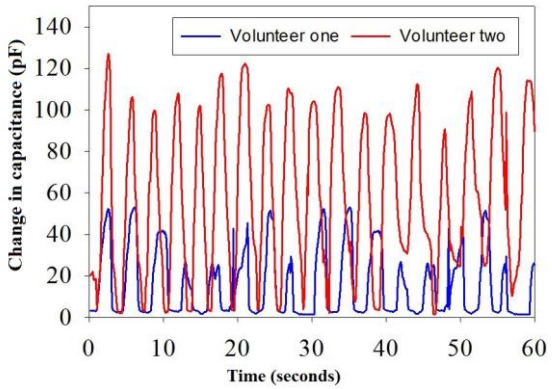

Fig. 20: Monitoring of respiration for two different individuals at rest.

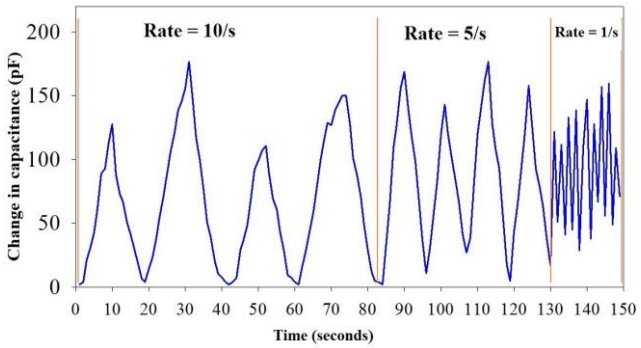

Fig. 21: Measurement of respiration activity of an individual who was simulating respiration rates of 10/s for the first 80s, 5/s for the next 45s and 1/s for the next 20s.

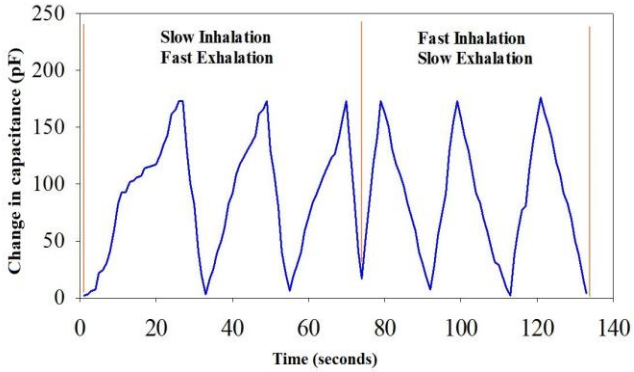

Fig. 22: Measurement of respiration activity of an individual who was simulating inhalation and exhalation at different speeds.

Table 1: Comparison of different force sensing resistors available in the market.

Sensor	Size (mm)	Force sensing capacity (lbs)	Price ($)	Application
RB-Phi-121	25*11	11.24	45.00	Pressure-sensitive touch user interface.
Flexiforce A101 Sensor	15.6 * 7.6	10	34.00	Bed monitoring systems, force sensitive video games.
SKU: SEN-09376	3.5	4.49	14.28	Tactile sensor for robotic appendages.
SEN-09375	2.375* 0.75*0.5	2.24	6.75	Bicycle handlebar glove, human symbiotic robot.

Table 2: Power and speed combinations of the laser cutting tool to obtain different electrode thicknesses.

Power (W)	**Speed (m/min)**	**z-axis (mm)**	**Thickness of the electrodes (microns)**
1.2	4.2	2	137
2.4	7	2	140
12	42	2	150
24	70	2	175
42	126	2	180